



# Performance analysis of G-MUSIC based DOA estimator with random linear array: A single source case



Han-Fei Zhou<sup>a,\*</sup>, Lei Huang<sup>a,\*</sup>, Hing Cheung So<sup>b</sup>, Jian Li<sup>c</sup>

<sup>a</sup>Institute of Multi-dimensional Signal Processing, College of Information Engineering, Shenzhen University, Shenzhen 518060, China

<sup>b</sup>Department of Electronic Engineering, City University of Hong Kong, Hong Kong, China

<sup>c</sup>Department of Electrical and Computer Engineering, University of Florida, Gainesville, FL 32611-6130, USA

## ARTICLE INFO

### Article history:

Received 20 April 2017

Revised 5 July 2017

Accepted 5 August 2017

Available online 7 August 2017

### Keywords:

Random linear array (RLA)

Direction-of-arrival (DOA)

Multiple signal classification (MUSIC)

Large random matrix theory (LRMT)

Consistent estimator

## ABSTRACT

We analyze the performance of direction-of-arrival (DOA) estimation based on the G-MUSIC algorithm for a single source using a random linear array, i.e., only a random subset of sensor array is in operation. The classical asymptotic analysis assumes that the number of snapshots tends to infinity whereas the number of sensors remains fixed. In contrast, this work studies the scenario where both quantities tend to infinity at the same rate. This general asymptotic regime provides a more accurate description of the practical situation where these two quantities are finite and comparable. We prove the consistency of the DOA estimator and derive an analytic expression for the mean square error (MSE) performance in the general asymptotic situation. The asymptotic MSE turns out to be a function of signal-to-noise ratio, probability of operating sensors and ratio of number of sensors to number of snapshots. Numerical results are presented to confirm the effectiveness of our theoretical calculations.

© 2017 Published by Elsevier B.V.

## 1. Introduction

Direction-of-arrival (DOA) estimation using a sensor array is required in many applications including radar, navigation and wireless communications. The uniform linear array (ULA) with maximum element spacing being less than half wavelength is widely assumed for this purpose. However, the sensors might be damaged or occluded by accident in practical applications. Therefore, it is interesting to determine the DOA parameters by utilizing a random linear array (RLA). On the whole, we assume that each sensor in the RLA is in operation with a known probability  $p$ .

For DOA estimation, subspace-based approaches are widely used because of their low complexity and robustness relative to the maximum-likelihood (ML) techniques, which are sensitive to signal and noise covariance matrix modeling errors [1–4]. Popular subspace-based algorithms for DOA estimation include Multiple Signal Classification (MUSIC) [5–9], and Estimating Signal Parameter via Rotational Invariance Techniques (ESPRIT) [10].

The philosophy behind the MUSIC approach [5–9] is based on a geometric understanding of received data, which partitions the observation space into two orthogonal subspaces. The first one is the so-called signal subspace which is in fact the column space of

steering matrix whereas its orthogonal complement is the noise subspace. Projecting the observed data onto the signal or noise subspace leads to the estimated locations of signals, namely, the DOA estimates. In particular, it casts the DOA estimation as an optimization problem, whose objective function involves the empirical estimate of the signal subspace projection matrix, which is formed using the rank- $K$  outer-product of the  $K$  leading eigenvectors of the sample covariance matrix (SCM), where  $K$  is the number of sources which is assumed known or estimated by an information theoretic criterion [11–13]. In this work, we consider  $K = 1$ , i.e., a single source case. Actually, the single-source situation has been studied by Suryaprakash et al. [14]. In their work, the consistency and mean square error (MSE) performance have been investigated with randomly missing data.

The problem of quantifying performance loss of MUSIC-based DOA estimation using a finite number of samples has been addressed in [1–4]. The closed-form expression for MSE of the MUSIC-based DOA estimator has been derived, which turns out to be a function of  $M$ ,  $N$  and signal-to-noise ratio (SNR). Herein,  $M$  and  $N$  stand for the number of sensors and number of snapshots, respectively. However, the statistical performance is only characterized in the situation where  $N$  tends to infinity while  $M$  remains finite. Indeed, under certain ergodicity assumptions and when  $N \rightarrow \infty$  for a fixed  $M$ , as it is called the classical asymptotic regime, the SCM converges almost surely to the population covariance matrix (PCM), and accordingly when  $N \gg M$  the sample

\* Corresponding author.

E-mail addresses: [hanfei\\_zhou@yeah.net](mailto:hanfei_zhou@yeah.net) (H.-F. Zhou), [luhuang@szu.edu.cn](mailto:luhuang@szu.edu.cn) (L. Huang).

eigenvectors tend to the accurate population eigenvectors. In practical applications, however,  $M$  is probably close to or even larger than  $N$ , which leads to strong discrepancies between the sample eigenvectors and their population counterparts. This originates what is usually referred to as the breakdown effect of subspace-based techniques [15]. In this case, the existing statistical analysis of the MUSIC-based DOA estimator is not correct any more and the MUSIC-based DOA estimator appears to be inconsistent [16].

However, it has been recently suggested that finite sample situations can be better examined by investigating the general asymptotic regime where  $M, N \rightarrow \infty$ ,  $M/N \rightarrow c$  where  $c$  is a constant greater than zero [17]. Based on the results in large random matrix theory (LRMT) [16,18], which is able to accurately determine the behaviours of the sample eigenvalues and eigenvectors in the general asymptotic regime, a G-MUSIC algorithm was derived in [17,19–22] to provide the consistent estimates of subspace in the general asymptotic regime. Therefore, the G-MUSIC based DOA estimator can guarantee consistency.

Unfortunately, the work in [16–19] cannot be applied directly to the consistency analysis of DOA estimation with RLA. The statistical behavior of the DOA estimator using G-MUSIC for RLA has not yet been investigated. This thereby motivates us to devote this work to the statistical performance analysis of the DOA estimator with RLA for a single source in the general asymptotic regime.

The contributions of this work are given as follows. 1) We show that for the situation of a single source with RLA, the DOA estimator based on the G-MUSIC algorithm is consistent in the general asymptotic regime provided that  $\text{SNR} \geq 1/(pM(\sqrt{M/c} - 1))$ . 2) For single source with RLA, we provide an analytic expression for the MSE of the DOA estimator, which turns out to be a function of SNR, probability  $p$  of operating sensors and ratio  $c$  of the number of sensors to the number of snapshots.

The rest of this paper is organized as follows. The system model and DOA estimator based on G-MUSIC algorithm are presented in Section 2. The consistency of the DOA estimator is established in Section 3. The closed-form expression for the MSE of the DOA estimator based on G-MUSIC is derived in Section 4. Numerical simulations used to validate our theoretical calculations are presented in Section 5 and concluding remarks are given in Section 6.

## 2. Preliminaries

### 2.1. Conventions

Most of domain dimensions (e.g.,  $M, N$ ) are denoted by capital Roman letters. Vectors and matrices are associated by bold symbols while lowercase letters are associated to scalar values. The transpose and conjugate transpose of a vector (or matrix)  $\mathbf{s}$  are denoted by  $\mathbf{s}^T$  and  $\mathbf{s}^H$ , respectively. The  $(i, j)$  component of a matrix  $\mathbf{P}$  is  $\mathbf{P}_{i,j}$ . The identity matrix is  $\mathbf{I}$ . The operator  $\mathbb{E}$  is the expectation operator. The real part and imaginary part of a complex number  $(\cdot)$  are denoted as  $\Re(\cdot)$  and  $\Im(\cdot)$ , respectively. The probability of the event  $(\cdot)$  is denoted as  $\mathbb{P}(\cdot)$ . The superscript  $(\cdot)'$  and  $(\cdot)''$  stand for the first-order and second-order derivatives, respectively. The  $\|\cdot\|_2$  represents the  $\ell_2$ -norm. The spectral radius of a matrix  $\mathbf{R}$  is denoted by  $\rho(\mathbf{R})$ . The  $\hat{\theta}_M \xrightarrow{P} \theta$  means the  $\hat{\theta}_M$  convergence to  $\theta$  in probability, and  $\hat{\theta}_M \xrightarrow{\text{a.s.}} \theta$  means  $\hat{\theta}_M$  almost-sure converges to  $\theta$ . For two functions  $g(M)$  and  $h(M)$ , we write  $g = \mathcal{O}(h)$  if  $|g| \leq c|h|$  for some constant  $c$  when  $M$  is sufficiently large.

### 2.2. Signal model with RLA

Consider a single source case where a narrowband signal with wavelength  $\lambda$  is incident from angle  $\theta$  on a RLA with  $M$  sensors of which the inter-element spacing is  $d\lambda$ , and each sensor is out

of operation with probability  $1 - p$ . The observation vector can be described by the following model:

$$\mathbf{y}(t) = x(t)\tilde{\mathbf{a}}(\theta) + \mathbf{e}(t), \quad t = 1, 2, \dots, N. \quad (1)$$

In (1),  $N$  is the number of snapshots,  $\mathbf{y}(t) \in \mathbb{C}^{M \times 1}$  is the observed data vector,  $x(t)$  is the signal waveform with zero mean, i.e.,  $\mathbb{E}[x(t)] = 0$ . Without loss of generality, we normalize the noise power, i.e.,  $\mathbf{e}(t) \in \mathbb{C}^{M \times 1}$  is an additive Gaussian white noise vector with zero mean and covariance matrix  $\mathbf{I}_M/M$ , then SNR can be expressed as  $\sigma^2 = \mathbb{E}[x(t)x^*(t)]$ . The steering vector of RLA has the following structure:

$$\tilde{\mathbf{a}}(\theta) = \mathbf{a}(\theta) \odot \mathbf{p} \quad (2)$$

where  $\odot$  denotes the Hadamard (element-wise) product,  $\mathbf{p} = [p_1, p_2, \dots, p_M]^T$  is the mask vector given by

$$p_m = \begin{cases} 1 & \text{with probability } p \\ 0 & \text{with probability } 1 - p \end{cases}$$

and  $\mathbf{a}(\theta) \in \mathbb{C}^{M \times 1}$  denotes the normalized steering vector of ULA with its  $m$ th element being given by

$$[\mathbf{a}(\theta)]_{m \in \mathcal{M}} = \frac{1}{\sqrt{M}} e^{j2\pi(m-1)d \sin \theta} \quad (3)$$

where  $\mathcal{M} = \{1, 2, \dots, M\}$ .

Let  $S \subseteq \mathcal{M}$  denote the support set of the random array manifold  $\tilde{\mathbf{a}}(\theta)$  and  $|S|$  be the cardinality of  $S$ . Moreover, the normalization of  $\tilde{\mathbf{a}}(\theta)$  is represented as  $\mathbf{s}(\theta)$  in which its  $m$ th element is

$$[\mathbf{s}(\theta)]_{m \in S} = \frac{1}{\sqrt{|S|}} e^{j2\pi(m-1)d \sin \theta} \quad (4)$$

with  $[\mathbf{s}(\theta)]_{m \in S^c} = 0$  for  $\forall m \in \mathcal{M}$  and  $\mathbb{P}\{m \in S\} = p$ .

### 2.3. DOA estimation based on G-MUSIC

For a specific array, i.e., a realization of the steering vector  $\mathbf{s}$ , the PCM of  $\mathbf{y}(t)$  is given by

$$\begin{aligned} \mathbf{R} &= \mathbb{E}[\mathbf{y}(t)\mathbf{y}^H(t)] = \sigma^2 \tilde{\mathbf{a}}(\theta)\tilde{\mathbf{a}}^H(\theta) + \frac{\mathbf{I}_M}{M} \\ &= \frac{|S|}{M} \sigma^2 \mathbf{s}(\theta)\mathbf{s}^H(\theta) + \frac{\mathbf{I}_M}{M} \end{aligned} \quad (5a)$$

$$= \sigma^2 \mathbf{A} \odot \mathbf{P} + \frac{\mathbf{I}_M}{M} \quad (5b)$$

where  $\mathbf{A} = \mathbf{a}(\theta)\mathbf{a}^H(\theta)$ , and  $\mathbf{P}$  is a symmetric mask random matrix given by

$$\mathbf{P}_{i,j|i=j} = \begin{cases} 1 & \text{with probability } p \\ 0 & \text{with probability } 1 - p \end{cases}$$

and

$$\mathbf{P}_{i,j|i>j} = \begin{cases} 1 & \text{with probability } p^2 \\ 0 & \text{with probability } 1 - p^2 \end{cases}$$

For notational convenience, we will simply write  $\tilde{\mathbf{a}}$  instead of  $\tilde{\mathbf{a}}(\theta)$ ,  $\mathbf{a}$  instead of  $\mathbf{a}(\theta)$  and  $\mathbf{s}$  instead of  $\mathbf{s}(\theta)$  whenever there is no possibility of confusion.

Let  $\lambda_1 \geq \lambda_2 \geq \dots \geq \lambda_M$  denote the eigenvalues of  $\mathbf{R}$  with non-increasing order. Since  $\text{rank}(\mathbf{s}\mathbf{s}^H) = 1$ , it follows that

$$\lambda_1 = \frac{|S|}{M} \sigma^2 + \frac{1}{M}, \quad (6a)$$

$$\lambda_m = \frac{1}{M}, \quad m = 2, 3, \dots, M. \quad (6b)$$

Then the unit-norm eigenvectors associated with  $\lambda_1$  is denoted by  $\mathbf{s}$ , and those corresponding to  $\lambda_2, \lambda_3, \dots, \lambda_M$  are denoted by  $\mathbf{g}_1, \mathbf{g}_2, \dots, \mathbf{g}_{M-1}$ . Setting

$$\mathbf{G} = [\mathbf{g}_1, \mathbf{g}_2, \dots, \mathbf{g}_{M-1}] \quad (7)$$

we have

$$\mathbf{s}^H \mathbf{G} \mathbf{G}^H \mathbf{s} = 0 \quad (8)$$

Since  $\mathbf{s} \mathbf{s}^H + \mathbf{G} \mathbf{G}^H = \mathbf{I}_M$ , (8) can also be written as

$$\mathbf{s}^H [\mathbf{I}_M - \mathbf{s} \mathbf{s}^H] \mathbf{s} = 0 \quad (9)$$

The idea behind the MUSIC algorithm is the exploitation of the orthogonal property (8) or (9). In practice,  $\mathbf{R}$  is unknown. Instead, its ML estimation, namely, the SCM is adopted, which is computed as

$$\hat{\mathbf{R}} = \frac{1}{N} \sum_{t=1}^N \mathbf{y}(t) \mathbf{y}^H(t). \quad (10)$$

Carrying out the eigendecomposition of  $\hat{\mathbf{R}}$ , we obtain the unit-norm sample eigenvectors  $\{\hat{\mathbf{s}}, \hat{\mathbf{g}}_1, \hat{\mathbf{g}}_2, \dots, \hat{\mathbf{g}}_{M-1}\}$ , which correspond to the non-increasing ordered sample eigenvalues  $\{\hat{\lambda}_1, \hat{\lambda}_2, \dots, \hat{\lambda}_M\}$ . Then the classical MUSIC algorithm returns  $\hat{\theta}^c$  by solving the optimization problem

$$\begin{aligned} \hat{\theta}^c &= \arg \max_{\phi \in \Phi} \frac{1}{\mathbf{s}^H(\phi) [\mathbf{I}_M - \hat{\mathbf{s}} \hat{\mathbf{s}}^H] \mathbf{s}(\phi)} \\ &= \arg \max_{\phi \in \Phi} \underbrace{\mathbf{s}^H(\phi) \hat{\mathbf{s}} \hat{\mathbf{s}}^H \mathbf{s}(\phi)}_{:= \hat{\mathcal{P}}^c(\phi)}, \text{ where } \Phi = \left[-\frac{\pi}{2}, \frac{\pi}{2}\right] \end{aligned} \quad (11)$$

where  $\hat{\mathcal{P}}^c(\phi)$  is the estimate of

$$\mathcal{P}^c(\phi) = \mathbf{s}^H(\phi) \mathbf{s}(\theta) \mathbf{s}^H(\theta) \mathbf{s}(\phi) \quad (12)$$

However, it has been revealed in [16] that  $\hat{\mathcal{P}}^c(\phi)$  in (11) is not  $M, N$ -consistent, that is, it fails to provide the consistent estimate of  $\mathcal{P}^c(\phi)$  in the general asymptotic regime. Consequently,  $\hat{\theta}^c$  is not an  $M, N$ -consistent estimate of  $\theta$  either. Moreover, the normalized random array manifold  $\mathbf{s}(\theta)$  of RLA is uncertain in the real-world measurement. In our work, the random manifold  $\mathbf{s}(\theta)$  of RLA is replaced by deterministic steering vector  $\mathbf{a}(\theta)$  to avoid estimating  $\mathbf{s}(\theta)$ , which yields the spectral function  $\mathcal{P}^U(\phi)$ . Motivated by G-MUSIC [16,18], we infer that  $\hat{\mathcal{P}}_M^U(\phi)$  is a consistent spectrum estimate of  $\mathcal{P}^U(\phi)$ , where

$$\mathcal{P}^U(\phi) = \mathbf{a}^H(\phi) \mathbf{s}(\theta) \mathbf{s}^H(\theta) \mathbf{a}(\phi) \quad (13)$$

and

$$\hat{\mathcal{P}}_M^U(\phi) = \mathbf{a}^H(\phi) \left( (1 + \mu) \hat{\mathbf{s}} \hat{\mathbf{s}}^H - \sum_{m=1}^{M-1} \nu(m) \hat{\mathbf{g}}_m \hat{\mathbf{g}}_m^H \right) \mathbf{a}(\phi) \quad (14)$$

where  $\mu$  and  $\nu$  are the functions of sample eigenvalues

$$\mu = \sum_{m=1}^{M-1} \left( \frac{\hat{\lambda}_{m+1}}{\hat{\lambda}_1 - \hat{\lambda}_{m+1}} - \frac{\hat{\kappa}_{m+1}}{\hat{\lambda}_1 - \hat{\kappa}_{m+1}} \right) \quad (15a)$$

$$\nu(m) = \frac{\hat{\lambda}_1}{\hat{\lambda}_{m+1} - \hat{\lambda}_1} - \frac{\hat{\kappa}_1}{\hat{\lambda}_{m+1} - \hat{\kappa}_1} \quad (15b)$$

in which  $\hat{\kappa}_1 \geq \hat{\kappa}_2 \geq \dots \geq \hat{\kappa}_M$  are the real-valued solutions to the following equality:

$$\frac{1}{M} \sum_{m=1}^M \frac{\hat{\lambda}_m}{\hat{\lambda}_m - \hat{\kappa}} = \frac{1}{c} \quad (16)$$

Consequently, the G-MUSIC algorithm for DOA estimation can be expressed as

$$\hat{\theta}_M = \arg \max_{\phi \in \Phi} \hat{\mathcal{P}}_M^U(\phi), \quad \Phi = \left[-\frac{\pi}{2}, \frac{\pi}{2}\right] \quad (17)$$

In next section, we will prove that  $\hat{\theta}_M$  is the  $M, N$ -consistent estimator of  $\theta$  in probability, which, to the best of our knowledge, has not yet been addressed in the literature.

### 3. Consistency of DOA estimator with RLA

Here we consider a system with RLA upon which a single narrow-band source impinges from the far field. We will prove that the DOA estimator (17) is  $M, N$ -consistent provided that SNR is not less than  $1/(pM(\sqrt{M/c} - 1))$ .

**Theorem 1** (Consistency). *Under  $0 < p < 1$ ,  $\sigma^2 > \frac{1}{pM(\sqrt{M/c} - 1)}$ , and as  $M, N$  tend to infinity at the same rate ( $M/N \rightarrow c$ ,  $0 < c < \infty$ ), then we have*

$$\hat{\theta}_M \xrightarrow{p} \theta$$

where  $\xrightarrow{p}$  means “convergence in probability”.

**Proof.** To prove Theorem 1 we first show in Proposition 1 that  $\hat{\mathcal{P}}_M^U(\phi)$  is a consistent estimate of  $\mathcal{P}^U(\phi)$  in the general asymptotic regime. The proof of this proposition is given in Appendix A.

**Proposition 1.** *Under  $0 < p < 1$ ,  $\sigma^2 > \frac{1}{pM(\sqrt{N-1})}$ , and as  $M, N \rightarrow \infty$ ,  $M/N \rightarrow c \in (0, \infty)$ , then we have*

$$\hat{\mathcal{P}}_M^U(\phi) \xrightarrow{a.s.} \mathcal{P}^U(\phi) \quad (18)$$

where  $\mathcal{P}^U(\phi)$  and  $\hat{\mathcal{P}}_M^U(\phi)$  are shown in (13) and (14) respectively.

Considering  $\mathbb{E}[\mathcal{P}^U(\phi)] = p\mathcal{P}^c(\phi)$ , we have

$$\hat{\mathcal{P}}_M^U(\phi) \xrightarrow{p} p\mathcal{P}^c(\phi) \quad (19)$$

as  $M \rightarrow \infty$ .

Without loss of generality, we prove the result for  $d = 1/2$ . The proof for  $d \neq 1/2$  follows in a similar manner. Let

$$\epsilon_M(\phi) = 1 - \mathcal{P}^c(\phi), \quad (20)$$

Then  $\theta$  is a solution to  $\epsilon_M(\phi) = 0$ . Similarly, let

$$\hat{\epsilon}(\phi) = 1 - \frac{1}{p} \hat{\mathcal{P}}_M^U(\phi). \quad (21)$$

Since  $\hat{\theta}_M$  is yielded by maximizing  $\hat{\mathcal{P}}_M^U(\phi)$ , we get  $|\hat{\epsilon}(\hat{\theta}_M)| \leq |\hat{\epsilon}(\theta)|$ . Moreover, since  $\hat{\epsilon}(\theta) \xrightarrow{p} \epsilon_M(\theta) = 0$ , we obtain  $\hat{\epsilon}(\hat{\theta}_M) \xrightarrow{p} 0$ . As a result, we have

$$|\epsilon_M(\hat{\theta}_M)| \leq |\epsilon_M(\hat{\theta}_M) - \hat{\epsilon}(\hat{\theta}_M)| + |\hat{\epsilon}(\hat{\theta}_M)| \xrightarrow{p} 0 \quad (22)$$

Since  $\epsilon_M(\hat{\theta}_M)$  depends on  $\mathcal{P}^c(\hat{\theta}_M)$ , we will now evaluate  $\mathcal{P}^c(\hat{\theta}_M)$ . Substituting the normalized RLA manifold (4) into (12), we have

$$\begin{aligned} \mathcal{P}^c(\hat{\theta}_M) &= \mathbf{s}^H(\hat{\theta}_M) \mathbf{s}(\theta) \mathbf{s}^H(\theta) \mathbf{s}(\hat{\theta}_M) \\ &= \left| \frac{1}{|\mathcal{S}|} \sum_{m \in \mathcal{S}} e^{j\pi(m-1)\varrho_M} \right|^2 \end{aligned} \quad (23)$$

where  $\varrho_M = \sin \theta - \sin \hat{\theta}_M$ . Since

$$\frac{1}{|\mathcal{S}|} \sum_{m \in \mathcal{S}} e^{j\pi(m-1)\varrho_M} \xrightarrow{p} \mathbb{E}[e^{j\pi(m-1)\varrho_M}] = \frac{1}{M} \sum_{m=1}^M e^{j\pi(m-1)\varrho_M}$$

it follows from [14] that

$$\sqrt{\mathcal{P}^c(\hat{\theta}_M)} \xrightarrow{p} \begin{cases} 0, & \text{if } \varrho_M \not\rightarrow 0; \\ 0, & \text{if } \varrho_M \rightarrow 0 \text{ and } M\varrho_M \rightarrow \infty; \\ \text{sinc}(\frac{\tau}{2}), & \text{if } \varrho_M \rightarrow 0 \text{ and } M\varrho_M \rightarrow \tau. \end{cases}$$

1. If  $\varrho_M \not\rightarrow 0$ ,  $\mathcal{P}^c(\hat{\theta}_M) \xrightarrow{p} 0$ ,  $\epsilon_M(\hat{\theta}_M) \xrightarrow{p} 1$ , which is contradicted with (22). Therefore,  $\varrho_M \rightarrow 0$ .

2. If  $\varrho_M \rightarrow 0$  but  $M\varrho_M \rightarrow \infty$ ,  $\mathcal{P}^c(\hat{\theta}_M) \xrightarrow{P} 0$ ,  $\epsilon_M(\hat{\theta}_M) \xrightarrow{P} 1$ , which is also contradicted with (22). Therefore,  $M\varrho_M$  is also bounded.
3. If  $\varrho_M \rightarrow 0$  and  $M\varrho_M \rightarrow \tau$ , then  $\mathcal{P}^c(\hat{\theta}_M) \xrightarrow{P} \text{sinc}^2(\tau/2)$ , this implies

$$\epsilon_M(\hat{\theta}_M) \xrightarrow{P} 1 - \text{sinc}^2\left(\frac{\tau}{2}\right), \text{ which is } \begin{cases} >0 & \text{if } \tau \neq 0; \\ =0 & \text{if } \tau = 0. \end{cases}$$

To avoid contradiction with (22),  $\tau = 0$ , so that  $M\varrho_M \xrightarrow{P} 0$ , which means that  $\sin \hat{\theta}_M \xrightarrow{P} \sin \theta$ , and thus  $\hat{\theta}_M \xrightarrow{P} \theta$  since  $\sin^{-1}(\cdot)$  is a continuous mapping.

In summary, under the general asymptotic regime,  $\hat{\theta}_M$  is an  $M$ ,  $N$ -consistent estimate of  $\theta$  in probability.  $\square$

#### 4. MSE of DOA estimator with RLA

Although the consistency of the DOA estimator based on G-MUSIC algorithm has been established in Section 3, we cannot theoretically evaluate its estimation accuracy. In this section, we address the DOA estimation error  $\Delta\theta := \hat{\theta}_M - \theta$ , from which we derive an approximate expression for the MSE of DOA estimator with RLA in the general asymptotic regime.

It follows from (17) that the G-MUSIC algorithm maximizes the objective function  $\hat{\mathcal{P}}_M^U(\phi)$ . Therefore, we have

$$\left. \frac{\partial \hat{\mathcal{P}}_M^U(\phi)}{\partial \phi} \right|_{\phi=\hat{\theta}_M} := (\hat{\mathcal{P}}_M^U)'(\hat{\theta}_M) = 0.$$

Expanding  $(\hat{\mathcal{P}}_M^U)'(\hat{\theta}_M)$  around  $\theta$  using Taylor formula yields

$$(\hat{\mathcal{P}}_M^U)'(\hat{\theta}_M) = (\hat{\mathcal{P}}_M^U)'(\theta) + (\Delta\theta)(\hat{\mathcal{P}}_M^U)''(\theta) + o(\Delta\theta)^2 = 0 \quad (24)$$

Since  $\hat{\theta}_M$  is the consistent estimator of  $\theta$ , we may neglect the  $o(\Delta\theta)^2$  terms to obtain the following approximation for  $\Delta\theta$  [23]:

$$\Delta\theta = -\frac{(\hat{\mathcal{P}}_M^U)'(\theta)}{(\hat{\mathcal{P}}_M^U)''(\theta)} \quad (25)$$

Differentiating  $\hat{\mathcal{P}}_M^U(\phi)$  with respect to  $\phi$  and evaluating the derivatives at  $\theta$ , we get

$$(\hat{\mathcal{P}}_M^U)'(\theta) = 2\Re\{\mathbf{a}^H(\theta)\hat{\mathbf{P}}_s\mathbf{a}'(\theta)\} \quad (26a)$$

$$(\hat{\mathcal{P}}_M^U)''(\theta) = 2\Re\{\mathbf{a}^H(\theta)\hat{\mathbf{P}}_s\mathbf{a}''(\theta)\} + 2(\mathbf{a}'(\theta))^H\hat{\mathbf{P}}_s\mathbf{a}'(\theta) \quad (26b)$$

where

$$\hat{\mathbf{P}}_s = (1 + \mu)\hat{\mathbf{S}}\hat{\mathbf{S}}^H - \sum_{m=1}^{M-1} \nu(m)\hat{\mathbf{g}}_m\hat{\mathbf{g}}_m^H \quad (27)$$

From (25), we get

$$\Delta\theta = -\frac{(1 + \mu)\delta_{\text{nu},1} - \delta_{\text{nu},2}}{(1 + \mu)\delta_{\text{de},1} - \delta_{\text{de},2} + (1 + \mu)\delta_{\text{de},3} - \delta_{\text{de},4}} \quad (28)$$

where

$$\delta_{\text{nu},1} = \Re\{\mathbf{a}^H(\theta)\hat{\mathbf{S}}\hat{\mathbf{S}}^H\mathbf{a}'(\theta)\} \quad (29a)$$

$$\delta_{\text{nu},2} = \sum_{m=1}^{M-1} \nu(m)\Re\{\mathbf{a}^H(\theta)\hat{\mathbf{g}}_m\hat{\mathbf{g}}_m^H\mathbf{a}'(\theta)\} \quad (29b)$$

$$\delta_{\text{de},1} = \Re\{\mathbf{a}^H(\theta)\hat{\mathbf{S}}\hat{\mathbf{S}}^H\mathbf{a}''(\theta)\} \quad (29c)$$

$$\delta_{\text{de},2} = \sum_{m=1}^{M-1} \nu(m)\Re\{\mathbf{a}^H(\theta)\hat{\mathbf{g}}_m\hat{\mathbf{g}}_m^H\mathbf{a}''(\theta)\} \quad (29d)$$

$$\delta_{\text{de},3} = |\mathbf{s}^H\mathbf{a}'(\theta)|^2 \quad (29e)$$

$$\delta_{\text{de},4} = \sum_{m=1}^{M-1} \nu(m)|\hat{\mathbf{g}}_m^H\mathbf{a}'(\theta)|^2 \quad (29f)$$

To proceed, we need to partition the manifold vector and its derivatives into signal and noise subspace components. That is

$$\mathbf{a}(\theta) = \gamma_0(\theta)\mathbf{s}(\theta) + \varpi_0(\theta)\mathbf{s}^\perp, \quad \varpi_0(\theta) \in \mathbb{R} \quad (30a)$$

$$\mathbf{a}'(\theta) = \gamma_1(\theta)\mathbf{s}(\theta) + \varpi_1(\theta)\mathbf{s}^\perp, \quad \varpi_1(\theta) \in \mathbb{R} \quad (30b)$$

$$\mathbf{a}''(\theta) = \gamma_2(\theta)\mathbf{s}(\theta) + \varpi_2(\theta)\mathbf{s}^\perp, \quad \varpi_2(\theta) \in \mathbb{R} \quad (30c)$$

where  $\mathbf{s}^\perp$  is a basis vector of the noise subspace orthogonal to the signal subspace, and

$$\gamma_0 = \sqrt{\frac{|S|}{M}}, \quad \varpi_0^2 = 1 - \frac{|S|}{M}; \quad (31a)$$

$$\gamma_1 = \langle \mathbf{s}(\theta), \mathbf{a}'(\theta) \rangle, \quad \varpi_1^2 = \|\mathbf{a}'(\theta)\|_2^2 - |\gamma_1|^2; \quad (31b)$$

$$\gamma_2 = \langle \mathbf{s}(\theta), \mathbf{a}''(\theta) \rangle, \quad \varpi_2^2 = \|\mathbf{a}''(\theta)\|_2^2 - |\gamma_2|^2. \quad (31c)$$

For notational simplicity, we have dropped  $\theta$  from (31) whenever there is no possibility of confusion.

Since  $\mathbf{s}^H(\theta)\mathbf{a}(\theta) = \sqrt{|S|/M}$ , differentiating both sides of this equality with respect to  $\theta$ , we obtain

$$\mathbf{s}^H(\theta)\mathbf{a}'(\theta) + (\mathbf{s}'(\theta))^H\mathbf{a}(\theta) = 0 \quad (32)$$

Since  $\mathbf{s}(\theta) = \sqrt{\frac{M}{|S|}}\mathbf{a}(\theta) \odot \mathbf{p}$ ,  $\mathbf{s}'(\theta) = \sqrt{\frac{M}{|S|}}\mathbf{a}'(\theta) \odot \mathbf{p}$ , we get

$$2\Re\{\mathbf{s}^H(\theta)\mathbf{a}'(\theta)\} = 2\Re\{\gamma_1\} = 0 \quad (33)$$

Substituting  $\mathbf{a}(\theta)$  and  $\mathbf{a}'(\theta)$  in (20), and considering (30), we get

$$\begin{aligned} \delta_{\text{nu},1} &= \Re\{(\gamma_0\mathbf{s}^H(\theta) + \varpi_0(\mathbf{s}^\perp)^H)\hat{\mathbf{S}}\hat{\mathbf{S}}^H(\gamma_1\mathbf{s}(\theta) + \varpi_1\mathbf{s}^\perp)\} \\ &= \Re\{\gamma_1\gamma_0|\mathbf{s}^H(\theta)\hat{\mathbf{S}}|^2 + \varpi_0\varpi_1|\hat{\mathbf{S}}^H\mathbf{s}^\perp|^2 \\ &\quad + \gamma_0\varpi_1\Re\{\mathbf{s}^H(\theta)\hat{\mathbf{S}}\hat{\mathbf{S}}^H\mathbf{s}^\perp\} + \varpi_0\Re\{\gamma_1(\mathbf{s}^\perp)^H\hat{\mathbf{S}}\hat{\mathbf{S}}^H\mathbf{s}(\theta)\} \\ &\quad + \underline{(a)}\varpi_0\varpi_1|\hat{\mathbf{S}}^H\mathbf{s}^\perp|^2 + \gamma_0\varpi_1\Re\{\mathbf{s}^H(\theta)\hat{\mathbf{S}}\hat{\mathbf{S}}^H\mathbf{s}^\perp\} \\ &\quad + (\varpi_0\Im\{\gamma_1\})\Im\{\mathbf{s}^H(\theta)\hat{\mathbf{S}}\hat{\mathbf{S}}^H\mathbf{s}^\perp\} \end{aligned} \quad (34)$$

Equality (a) results from  $\Im\{(\mathbf{s}^\perp)^H\hat{\mathbf{S}}\hat{\mathbf{S}}^H\mathbf{s}(\theta)\} + \Im\{\mathbf{s}^H(\theta)\hat{\mathbf{S}}\hat{\mathbf{S}}^H\mathbf{s}^\perp\} = 0$  and  $\Re\{\gamma_1\} = 0$ .

For  $m = 1, 2, \dots, M-1$ , let

$$\alpha_0 = \mathbf{s}^H(\theta)\hat{\mathbf{S}}, \quad \beta_0 = \hat{\mathbf{S}}^H\mathbf{s}^\perp, \quad (35a)$$

$$\alpha_m = \mathbf{s}^H(\theta)\hat{\mathbf{g}}_m, \quad \beta_m = \hat{\mathbf{g}}_m^H\mathbf{s}^\perp. \quad (35b)$$

Since it is indicated in (B.1e) that  $\alpha_0\beta_0 \xrightarrow{\text{a.s.}} 0$ ,  $\delta_{\text{nu},1}$  can be rewritten as

$$\delta_{\text{nu},1} = \varpi_0\varpi_1|\beta_0|^2 \quad (36)$$

Adopting the similar manipulations, we get

$$\delta_{\text{nu},2} = \sum_{m=1}^{M-1} \nu(m)\varpi_0\varpi_1|\beta_m|^2 \quad (37a)$$

$$\delta_{\text{de},1} = \gamma_0\Re\{\gamma_2\}|\alpha_0|^2 + \varpi_0\varpi_2|\beta_0|^2 \quad (37b)$$

$$\delta_{\text{de},2} = \sum_{m=1}^{M-1} \nu(m) \left( \gamma_0 \Re\{\gamma_2\} |\alpha_m|^2 + \varpi_0 \varpi_2 |\beta_m|^2 \right) \quad (37c)$$

$$\delta_{\text{de},3} = |\gamma_1|^2 |\alpha_0|^2 + \varpi_1^2 |\beta_0|^2 \quad (37d)$$

$$\delta_{\text{de},4} = \sum_{m=1}^{M-1} \nu(m) \left( |\gamma_1|^2 |\alpha_m|^2 + \varpi_1^2 |\beta_m|^2 \right) \quad (37e)$$

From Lemma 2 and (C.5), we obtain

$$|\alpha_0|^2 = \mathcal{O}(1), \quad |\beta_0|^2 = \mathcal{O}(M^{-2}); \quad (38a)$$

$$|\alpha_m|^2 = \mathcal{O}(M^{-2}), \quad |\beta_m|^2 = \mathcal{O}(M^{-1}); \quad (38b)$$

$$\gamma_0 = \mathcal{O}(1), \quad \varpi_0 = \mathcal{O}(1); \quad (38c)$$

$$\Im\{\gamma_1\} = |\gamma_1| = \mathcal{O}(M), \quad \varpi_1 = \mathcal{O}(M); \quad (38d)$$

$$\Re\{\gamma_2\} = \mathcal{O}(M^2), \quad \Im\{\gamma_2\} = \mathcal{O}(M); \quad (38e)$$

$$\varpi_2 = \mathcal{O}(M^2). \quad (38f)$$

Recalling (36) and (37), we have

$$\delta_{\text{nu},1} = \varpi_0 \varpi_1 |\beta_0|^2 \quad (39a)$$

$$\delta_{\text{nu},2} = \varpi_0 \varpi_1 \sum_{m=1}^{M-1} \nu(m) |\beta_m|^2 \quad (39b)$$

$$\delta_{\text{de},1} \approx \gamma_0 \Re\{\gamma_2\} |\alpha_0|^2 \quad (39c)$$

$$\delta_{\text{de},2} \approx \gamma_0 \Re\{\gamma_2\} \sum_{m=1}^{M-1} \nu(m) |\alpha_m|^2 \quad (39d)$$

$$\delta_{\text{de},3} \approx |\gamma_1|^2 |\alpha_0|^2 \quad (39e)$$

$$\delta_{\text{de},4} \approx \varpi_1^2 \sum_{m=1}^{M-1} \nu(m) |\beta_m|^2 \quad (39f)$$

Considering  $\mu = \sum_{m=1}^{M-1} \nu(m)$  in [16], we define

$$\check{\delta}_{\text{nu}} = |\beta_0|^2 + \sum_{m=1}^{M-1} \nu(m) (|\beta_0|^2 - |\beta_m|^2) \quad (40a)$$

$$\check{\delta}_{\text{de},1} = |\alpha_0|^2 + \sum_{m=1}^{M-1} \nu(m) (|\alpha_0|^2 - |\alpha_m|^2) \quad (40b)$$

$$\check{\delta}_{\text{de},2} = |\alpha_0|^2 \quad (40c)$$

$$\check{\delta}_{\text{de},3} = \sum_{m=1}^{M-1} \nu(m) |\beta_m|^2 \quad (40d)$$

Since  $\check{\delta}_{\text{de},3}/\check{\delta}_{\text{de},1} = o(M^{-1})$ , and considering (28), (39) and (40), we obtain

$$[\Delta\theta]^2 \approx \frac{\varpi_0^2 \varpi_1^2 \check{\delta}_{\text{nu}}^2}{\gamma_0^2 \Re\{\gamma_2\} \check{\delta}_{\text{de},1}^2 + |\gamma_1|^4 \check{\delta}_{\text{de},2}^2 + 2\gamma_0 \Re\{\gamma_2\} |\gamma_1|^2 \check{\delta}_{\text{de},1} \check{\delta}_{\text{de},2}} \quad (41)$$

Then from (C.5), we get

$$\mathbb{E}[\Delta\theta]^2 \approx \frac{1-p}{3M^2\pi^2 d^2 \cos^2 \theta} \frac{\check{\delta}_{\text{nu}}^2}{(\frac{4}{3}\sqrt{p}\check{\delta}_{\text{de},1} - \check{\delta}_{\text{de},2})^2}$$

$$\triangleq \frac{1-p}{3M^2\pi^2 d^2 \cos^2 \theta} \frac{\check{\delta}_{\text{nu}}^2}{\check{\delta}_{\text{de}}^2} \quad (42)$$

where

$$\begin{aligned} \check{\delta}_{\text{de}} &= \frac{4}{3}\sqrt{p}\check{\delta}_{\text{de},1} - \check{\delta}_{\text{de},2} \\ &= (\frac{4}{3}\sqrt{p} - 1)|\alpha_0|^2 + \frac{4}{3}\sqrt{p} \sum_{m=1}^{M-1} \nu(m) (|\alpha_0|^2 - |\alpha_m|^2) \end{aligned} \quad (43)$$

Hence

$$\frac{\check{\delta}_{\text{nu}}}{\check{\delta}_{\text{de}}} \rightarrow -\frac{\sum_{m=1}^{M-1} \nu(m) |\beta_m|^2}{\frac{4}{3}\sqrt{p}\mu |\alpha_0|^2} \rightarrow \frac{(1 - \frac{c}{pM^2\sigma^2})}{\frac{4}{3}\sqrt{p}M(1 - \frac{c}{pM\sigma^2})} \quad (44)$$

Consequently, it follows from (42) that

$$\mathbb{E}[\Delta\theta]^2 \approx \frac{1}{(1 - \frac{c}{pM\sigma^2})^2} \frac{3(1-p)}{16p} \frac{1}{M^4\pi^2 d^2 \cos^2 \theta} \quad (45)$$

for  $0 < p < 1$ , as  $M, N \rightarrow \infty$ ,  $M/N \rightarrow c \in (0, \infty)$ .

The analytic expression (45) for the MSE performance turns out to be a function of SNR ( $\sigma^2$ ), probability  $p$  of operating sensors and ratio  $c$  of number of sensors to number of snapshots.

## 5. Experiments

In this section, we evaluate the performance of G-MUSIC algorithm for DOA estimation with RLA. In particular, we firstly compare the spectrum estimate of the RLA to that of ULA with the same numbers of sensors and snapshots. Secondly, we examine the consistency of the G-MUSIC algorithm in the general asymptotic regime. Finally, the empirical MSE is compared with its theoretical calculations for the classical and general asymptotic regimes.

### 5.1. Spectrum estimation

In this example, the DOA of the single source is  $25^\circ$  and its SNR is  $-5$  dB. Fig. 1 plots the spatial spectra for RLA and ULA. The parameter settings for these two arrays are the same but each sensor in the RLA is operating with probability of 0.5, namely,  $p = 0.5$ . The inter-element spacing is  $d/\lambda = 1/2$ , the number of sensors varies from 20, 30, 40 to 50. The ratio of number of sensors to number of snapshots is  $c = 0.5$ . It is indicated in Fig. 1 that the RLA with half sensors out of operation is still able to obtain the similar spatial spectra as the ULA of which all sensors are in operation.

### 5.2. Consistency of DOA estimator

Let us now examine the consistency of the G-MUSIC algorithm for DOA estimation. The correct ratio is defined as the ratio of number of accurate estimation to the total experiment times, where an accurate estimate is evaluated by thresholding  $|\Delta\theta| \leq 1/(2Md)$ . For each  $M$ , we carry out 500 Monte Carlo runs. In the first experiment, we set SNR =  $-5$  dB and  $p = 0.2$ , the ratio  $c$  of number of sensors to number of snapshots is varying from 0.5, 1.0 to 2.0. The empirical results are plotted in Fig. 2a, which imply that the DOA estimator is able to converge to 1.0 in terms of correct ratio. Besides, as  $c = M/N$  becomes smaller ( $N$  is much larger than  $M$ ), the convergence becomes faster, which agrees well with the classical estimation theory. In the second experiment, we set  $c = 2$  and  $p = 0.4$ , the SNR is varying from  $-12$  dB,  $-6$  dB to 0 dB. The empirical results are plotted in Fig. 2b, which imply again that the DOA estimator is able to converge to 1.0 in terms of correct ratio for different SNR.



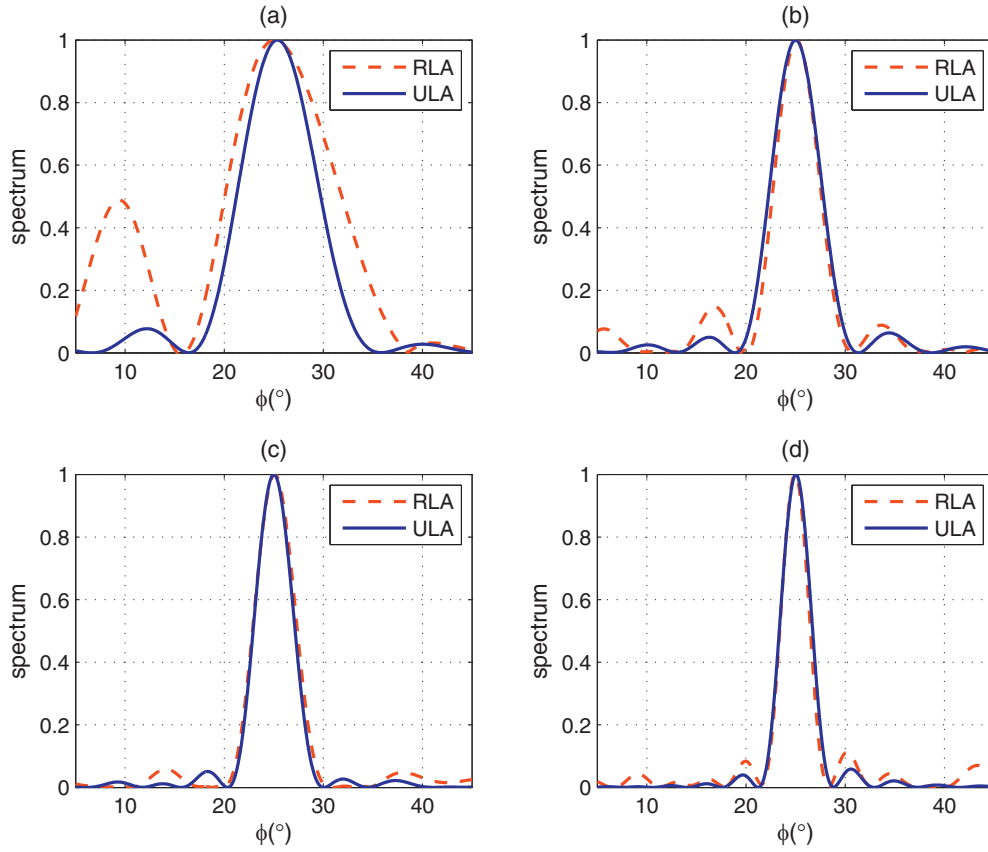


Fig. 1. Spatial spectra of RLA and ULA. (a)  $M=20$ ,  $N=40$ ; (b)  $M=30$ ,  $N=60$ ; (c)  $M=40$ ,  $N=80$ ; (d)  $M=50$ ,  $N=100$ .

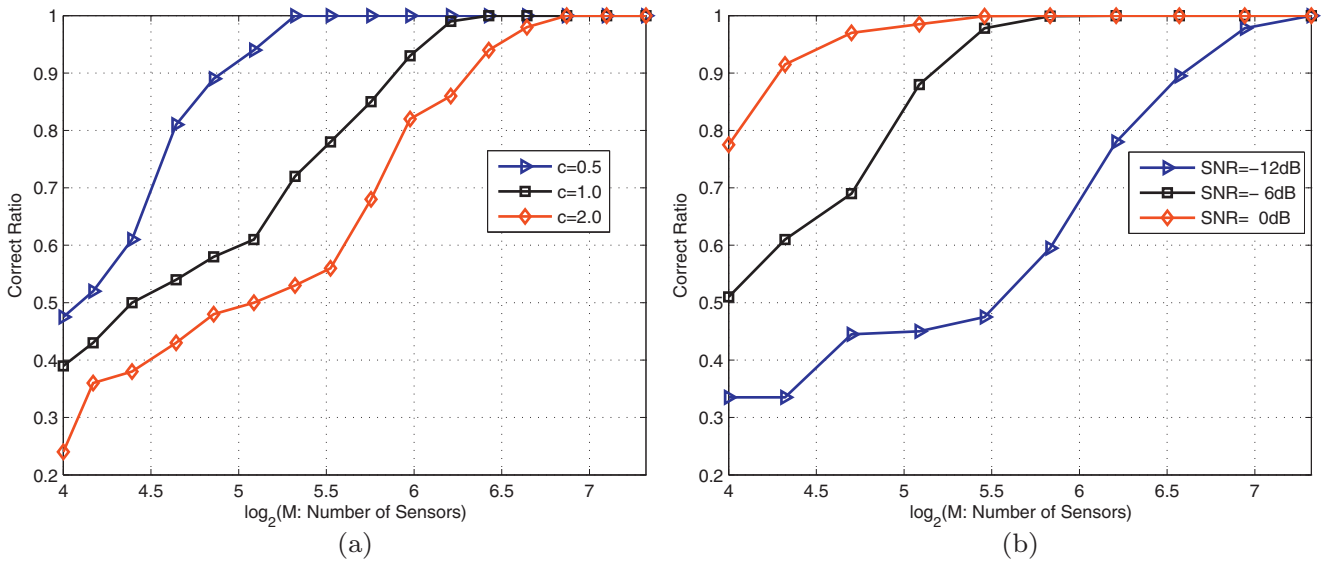


Fig. 2. Correct ratio versus number of sensors. (a) The ratio  $c$  is varying from 0.5, 1.0 to 2.0; (b) The SNR is varying from -12dB, -6dB to 0dB.

### 5.3. MSE Of DOA estimator

In this simulation, we vary the ratio  $c = M/N$  from 0.5, 2.0 to 5.0,  $\text{SNR} = -5\text{ dB}$  or  $5\text{ dB}$ , and the probability  $p$  is varying from 0.125, 0.5 to 0.9. The empirical MSE of each  $M$  is averaged from 500 Monte Carlo trials, which is depicted in Fig. 3. For comparison, the corresponding theoretical MSE, expressed by (45), is provided as well. It is observed that the theoretical expression of MSE is accurate when  $M$  and  $N$  become relatively large.

## 6. Conclusion

In this paper, we have theoretically analyzed the statistical performance of the G-MUSIC algorithm for single source DOA estimation with RLA. Using recent results from RMT, we have shown that the proposed DOA estimator is consistent as  $M, N$  tend to infinity and  $0 < c = M/N < \infty$  for  $p \in (0, 1)$ . Furthermore, we have derived the analytical expression for the MSE of this DOA estimator, and validated our theoretical computations via simulation results.

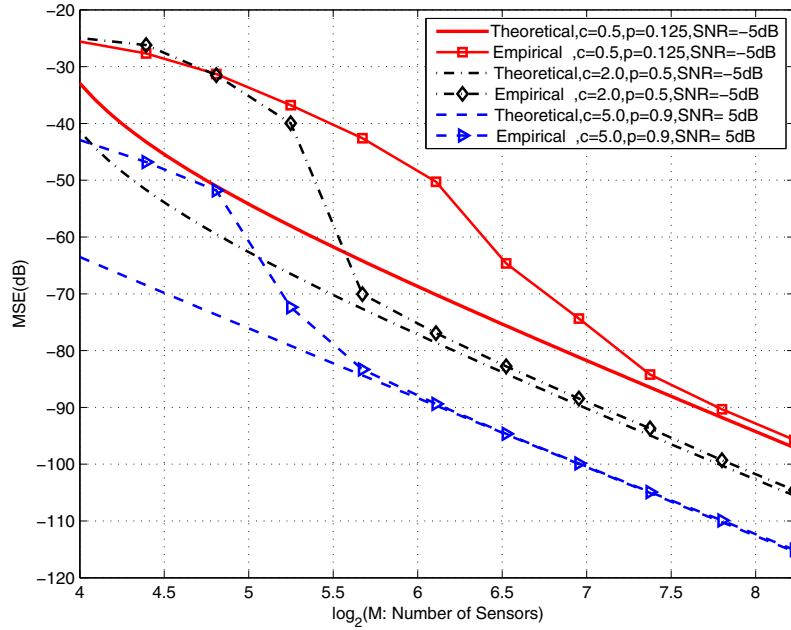


Fig. 3. MSE of DOA estimator based on G-MUSIC algorithm for RLA: empirical vs theoretical.

For multiple sources with RLA, it is quite difficult to theoretically prove the consistency of the estimator, so does the MSE calculation. This is our future work.

### Acknowledgments

The work described in this paper was supported by the National Natural Science Foundation of China under Grants U1501253, the Natural Science foundation of Guangdong Province, P.R. China (No. 2015A030311030), the Foundation of Shenzhen City under Grant ZDSYS201507081625213 and the Foundation of Nanshan District Shenzhen City under Grant KC2015ZDYF0023A.

### Appendix A. Proof of Proposition 1

In order to prove that  $\hat{\mathcal{P}}_M^U(\phi)$  is an  $M, N$ -consistent estimate of  $\mathcal{P}^U(\phi)$ , we need the following results about the eigenvalues distribution of the PCM.

**Lemma 1.** Let  $\lambda_1 = p\sigma^2 + \frac{1}{M} > \lambda_2 = \lambda_3 = \dots = \lambda_M = \frac{1}{M}$  denote the eigenvalues of  $\mathbf{R}$  and  $\bar{f}$  denotes the smallest real-valued solution for  $f$  to the following equality

$$\frac{1}{M} \sum_{m=1}^M \frac{\lambda_m^2}{(\lambda_m - f)^3} = 0 \quad (\text{A.1})$$

Then for  $0 < p < 1$ ,  $\sigma^2 > \frac{1}{pM(\sqrt{N}-1)}$  as  $M, N \rightarrow \infty$ ,  $M/N \rightarrow c \in (0, \infty)$ , we get  $\zeta < 1/c$ , where

$$\zeta := \frac{1}{M} \sum_{m=1}^M \frac{\lambda_m^2}{(\lambda_m - \bar{f})^2} \quad (\text{A.2})$$

**Proof.** Note that (A.1) is equivalent to

$$\frac{\lambda_1^2}{(\lambda_1 - \bar{f})^3} = \frac{(M-1)\lambda_2^2}{(\bar{f} - \lambda_2)^3} \quad (\text{A.3})$$

Solving (A.3), we get a real-valued solution given as

$$\bar{f} = \lambda_2 + \frac{\lambda_1 - \lambda_2}{1 + \left(\frac{\lambda_1^2}{(M-1)\lambda_2^2}\right)^{1/3}} \quad (\text{A.4})$$

On the other hand, (A.3) can be rewritten as

$$\frac{1}{M} \frac{\lambda_1^2}{(\lambda_1 - \bar{f})^2} = \frac{(M-1)(\lambda_1 - \bar{f})\lambda_2^2}{M(\bar{f} - \lambda_2)^3} \quad (\text{A.5})$$

Thus, we obtain

$$\begin{aligned} \zeta &:= \frac{1}{M} \frac{\lambda_1^2}{(\lambda_1 - \bar{f})^2} + \frac{M-1}{M} \frac{\lambda_2^2}{(\bar{f} - \lambda_2)^2} \\ &= \frac{(M-1)(\lambda_1 - \bar{f})\lambda_2^2}{M(\bar{f} - \lambda_2)^3} + \frac{M-1}{M} \frac{\lambda_2^2}{(\bar{f} - \lambda_2)^2} \\ &= \frac{M-1}{M} \frac{\lambda_2^2(\lambda_1 - \lambda_2)}{(\bar{f} - \lambda_2)^3} \\ &\rightarrow \frac{(1 + \frac{1}{pM\sigma^2})^2}{M} < \frac{1}{c} = \frac{N}{M}, \end{aligned} \quad (\text{A.6})$$

for  $\sigma^2 > \frac{1}{pM(\sqrt{N}-1)}$  or  $\sigma^2 > \frac{1}{pM(\sqrt{M/c}-1)}$ .  $\square$

It is shown in [16] that  $\hat{\mathcal{P}}_M^U(\phi)$  is an  $M, N$ -consistent estimator of  $\mathcal{P}^U(\phi)$ , that is

$$\hat{\mathcal{P}}_M^U(\phi) \xrightarrow{\text{a.s.}} \mathcal{P}^U(\phi) \quad (\text{A.7})$$

as the population and sample covariance matrices, i.e.,  $\mathbf{R}$  and  $\hat{\mathbf{R}}$ , satisfy the following four properties:

- 1) The PCM  $\mathbf{R}$  has uniformly bounded spectral norm, namely,  $\rho(\mathbf{R}) < +\infty$ . This property is satisfied because  $\lambda_{\max} = \lambda_1 < \sigma^2 + 1$ .
- 2) The deterministic steering vector  $\mathbf{a}(\phi)$  has uniformly bounded norm since  $\|\mathbf{a}(\phi)\|_2 = 1$ .
- 3) The SCM takes the form  $\hat{\mathbf{R}} = \mathbf{R}^{1/2} \mathbf{U} \mathbf{U}^H \mathbf{R}^{1/2}$ , where  $\mathbf{R}^{1/2}$  is a positive-definite Hermitian square-root of the PCM  $\mathbf{R}$ , and  $\mathbf{U}$  is an  $M \times N$  matrix with complex i.i.d. absolutely continuous random entries, each of which has i.i.d. real and imaginary parts with zero mean and variance  $1/2N$ . Let  $\mathbf{y}(t) = \sqrt{N} \mathbf{R}^{1/2} \mathbf{u}(t)$ ,  $\mathbf{U} = [\mathbf{u}(1), \mathbf{u}(2), \dots, \mathbf{u}(t), \dots, \mathbf{u}(N)]$  where

$$\mathbf{u}(t) = \frac{1}{\sqrt{N}} \mathbf{R}^{-1/2} \mathbf{y}(t), \quad t = 1, 2, \dots, N. \quad (\text{A.8})$$

Then,  $\hat{\mathbf{R}}$  and  $\mathbf{U}$  have the properties as aforementioned.

- 4) If  $\lambda_1, \lambda_2, \dots, \lambda_M$  are the eigenvalues of the PCM  $\mathbf{R}$ , then  $\zeta < 1/c$ , where  $\zeta$  is defined in (A.2). In Lemma 1, we have proved that the PCM has the property for  $0 < p < 1$ ,  $\sigma^2 > \frac{1}{pM(\sqrt{N}-1)}$ , as  $M, N \rightarrow \infty, M/N \rightarrow c \in (0, \infty)$ .

In summary, under  $0 < p < 1$ ,  $\sigma^2 > \frac{1}{pM(\sqrt{N}-1)}$ , as  $M \rightarrow \infty, M/N \rightarrow c \in (0, \infty)$ ,  $\hat{\mathcal{P}}_M^{\mathbf{U}}(\phi)$  is a  $M, N$ -consistent estimator of  $\mathcal{P}^{\mathbf{U}}(\phi)$ .

## Appendix B. Lemma for Proof of (36) and (37)

From (36) and (37), we note that characterizing  $\alpha_0, \beta_0, \{\alpha_m\}_{m=1}^{M-1}$  and  $\{\beta_m\}_{m=1}^{M-1}$  of (35), which quantifies the accuracy of the sample eigenvector relative to the population eigenvector, is critical to analyzing the MSE performance. In this appendix, we present a characterization of these terms of RLA in the general asymptotic regime, i.e.,  $0 < p < 1$ ,  $M, N \rightarrow \infty, \frac{M}{N} \rightarrow c \in (0, \infty)$ , and  $\text{SNR} = \sigma^2 > \frac{1}{pM(\sqrt{M/c}-1)}$ .

**Lemma 2.** When  $0 < p < 1$ , suppose  $p\sigma^2 + \frac{1}{M} = \lambda_1 > \frac{1}{M} = \lambda_2 = \dots = \lambda_M$  and  $\{\mathbf{s}, \mathbf{G}\} (\mathbf{G} = \{\mathbf{g}_1, \mathbf{g}_2, \dots, \mathbf{g}_{M-1}\})$  are the eigenvalues and eigenvectors of PCM  $\mathbf{R}$ , and  $\hat{\mathbf{R}}, \hat{\lambda}_1 \geq \hat{\lambda}_2 \geq \dots \geq \hat{\lambda}_M$  and  $\{\hat{\mathbf{s}}, \hat{\mathbf{G}}\}$  denote the SCM, sample eigenvalues and sample eigenvectors, respectively. As a result, we obtain

$$|\alpha_0|^2 \xrightarrow{\text{a.s.}} 1 - \frac{c}{pM\sigma^2} \quad (\text{B.1a})$$

$$\sum_{m=1}^{M-1} |\alpha_m|^2 \xrightarrow{\text{a.s.}} \frac{c}{pM\sigma^2} \quad (\text{B.1b})$$

$$|\beta_0|^2 \xrightarrow{\text{a.s.}} \frac{c}{pM^2\sigma^2} \quad (\text{B.1c})$$

$$\sum_{m=1}^{M-1} |\beta_m|^2 \xrightarrow{\text{a.s.}} 1 - \frac{c}{pM^2\sigma^2} \quad (\text{B.1d})$$

$$\alpha_0\beta_0 \xrightarrow{\text{a.s.}} 0 \quad (\text{B.1e})$$

$$\alpha_m\beta_m \xrightarrow{\text{a.s.}} 0 \quad (\text{B.1f})$$

as  $M, N \rightarrow \infty$  at the same rate ( $M/N \rightarrow c, 0 < c < \infty$ ), where  $\alpha_0, \beta_0$  and  $\{\alpha_m, \beta_m\}_{m=1}^{M-1}$  are defined in (35).

**Proof.** Let  $\kappa_1 \geq \kappa_2$  be the solution to the following equality in  $\kappa$ :

$$\frac{1}{M} \frac{\lambda_1}{\lambda_1 - \kappa} + \frac{M-1}{M} \frac{\lambda_2}{\lambda_2 - \kappa} = \frac{1}{c}, \quad (\text{B.2})$$

then we obtain

$$\kappa_1 \approx \lambda_1 - \frac{c}{M}(\lambda_1 - \lambda_2) - \frac{c}{M}(\lambda_1 - \lambda_2)(1-c)\lambda_2 \quad (\text{B.3a})$$

$$\kappa_2 \approx (1-c)\lambda_2 + \frac{c}{M}(\lambda_1 - \lambda_2)(1-c)\lambda_2 \quad (\text{B.3b})$$

According to Theorem 2 in [16], we get

$$|\alpha_0|^2 = \mathbf{s}^H(\theta) \hat{\mathbf{S}} \hat{\mathbf{S}}^H \mathbf{s}(\theta) \xrightarrow{\text{a.s.}} \varsigma_1 \quad (\text{B.4a})$$

$$\sum_{m=1}^{M-1} |\alpha_m|^2 = \mathbf{s}^H(\theta) \hat{\mathbf{G}} \hat{\mathbf{G}}^H \mathbf{s}(\theta) \xrightarrow{\text{a.s.}} \varsigma_2 \quad (\text{B.4b})$$

where

$$\varsigma_1 = 1 - (M-1) \left( \frac{\lambda_1}{\lambda_2 - \lambda_1} - \frac{\kappa_1}{\lambda_2 - \kappa_1} \right) \quad (\text{B.5a})$$

$$\varsigma_2 = \frac{\lambda_2}{\lambda_1 - \lambda_2} - \frac{\kappa_2}{\lambda_1 - \kappa_2} \quad (\text{B.5b})$$

Considering  $\lambda_1 = p\sigma^2 + \frac{1}{M}, \lambda_2 = \frac{1}{M}$  and  $\kappa_1, \kappa_2$  in (B.3), we get

$$|\alpha_0|^2 \xrightarrow{\text{a.s.}} \varsigma_1 \rightarrow 1 - \frac{c}{pM\sigma^2} \quad (\text{B.6a})$$

$$\sum_{m=1}^{M-1} |\alpha_m|^2 \xrightarrow{\text{a.s.}} \varsigma_2 \rightarrow \frac{c}{pM\sigma^2} \quad (\text{B.6b})$$

Since  $\mathbf{s}^\perp$  is a basis vector of the noise subspace orthogonal to the signal subspace, we have  $\mathbf{s}^H \mathbf{s}^\perp = 0$  and  $\|\mathbf{G}^H \mathbf{s}^\perp\|_2 = 1$ . Utilizing similar manipulations, we get

$$|\beta_0|^2 \xrightarrow{\text{a.s.}} \varsigma_3^t (\mathbf{s}^\perp)^H \mathbf{S} \mathbf{S}^H \mathbf{s}^\perp + \varsigma_3 (\mathbf{s}^\perp)^H \mathbf{G} \mathbf{G}^H \mathbf{s}^\perp = \varsigma_3 \quad (\text{B.7a})$$

$$\sum_{m=1}^{M-1} |\beta_m|^2 \xrightarrow{\text{a.s.}} \varsigma_4 (\mathbf{s}^\perp)^H \mathbf{G} \mathbf{G}^H \mathbf{s}^\perp + \varsigma_4^t (\mathbf{s}^\perp)^H \mathbf{S} \mathbf{S}^H \mathbf{s}^\perp = \varsigma_4 \quad (\text{B.7b})$$

$$\alpha_0\beta_0 \xrightarrow{\text{a.s.}} \varsigma_5^t \mathbf{s}^H \mathbf{S} \mathbf{S}^H \mathbf{s}^\perp + \varsigma_5 \mathbf{s}^H \mathbf{G} \mathbf{G}^H \mathbf{s}^\perp = 0 \quad (\text{B.7c})$$

$$\alpha_m\beta_m \xrightarrow{\text{a.s.}} \varsigma_6^{t_1} \mathbf{s}^H \mathbf{S} \mathbf{S}^H \mathbf{s}^\perp + \varsigma_6^{t_2} \mathbf{s}^H \mathbf{g}_m \mathbf{g}_m^H \mathbf{s}^\perp + \varsigma_6 \mathbf{s}^H \bar{\mathbf{G}}_m \bar{\mathbf{G}}_m^H \mathbf{s}^\perp = 0 \quad (\text{B.7d})$$

where  $\bar{\mathbf{G}}_m = [\mathbf{g}_1, \mathbf{g}_2, \dots, \mathbf{g}_{m-1}, \mathbf{g}_{m+1}, \dots, \mathbf{g}_{M-1}]$  and

$$\varsigma_3 = \frac{\lambda_1}{\lambda_2 - \lambda_1} - \frac{\kappa_1}{\lambda_2 - \kappa_1} \quad (\text{B.8a})$$

$$\varsigma_4 = 1 - \frac{1}{M-1} \left( \frac{\lambda_2}{\lambda_1 - \lambda_2} - \frac{\kappa_2}{\lambda_1 - \kappa_2} \right) \quad (\text{B.8b})$$

Similarly, we get

$$|\beta_0|^2 \xrightarrow{\text{a.s.}} \varsigma_3 \rightarrow \frac{c}{pM^2\sigma^2} \quad (\text{B.9a})$$

$$\sum_{m=1}^{M-1} |\beta_m|^2 \xrightarrow{\text{a.s.}} \varsigma_4 \rightarrow 1 - \frac{c}{pM^2\sigma^2} \quad (\text{B.9b})$$

□

## Appendix C. Manifold vector scaling of RLA

In this appendix, we will compute manifold vector terms including  $\gamma_0, \gamma_1, \gamma_2, \varpi_0, \varpi_1$  and  $\varpi_2$  in (30), which are used in the derivations of the MSE expression of DOA estimator. The  $m$ th ( $m = 1, 2, \dots, M$ ) element of the first derivative of  $\mathbf{a}(\theta)$  evaluated at  $\theta$  is

$$[\mathbf{a}'(\theta)]_m = j2\pi d \cos \theta \frac{m-1}{\sqrt{M}} e^{j2\pi d(m-1) \sin \theta} \quad (\text{C.1})$$

Using (4), (30), (31) and (C.1), we have

$$\mathcal{I}\{\gamma_1\} = \frac{2\pi d \cos \theta}{\sqrt{M}} \sum_{m \in \mathcal{S}} \frac{m-1}{\sqrt{|S|}} \quad (\text{C.2a})$$

$$|\gamma_1|^2 = \frac{4\pi^2 d^2 \cos^2 \theta}{M} \frac{\left[ \sum_{m \in \mathcal{S}} (m-1) \right]^2}{|S|} \quad (\text{C.2b})$$

$$\|\mathbf{a}'(\theta)\|_2^2 = \frac{4\pi^2 d^2 \cos^2 \theta}{M} \sum_{m=1}^M (m-1)^2 \quad (\text{C.2c})$$



$$\varpi_1^2 = \|\mathbf{a}'(\theta)\|_2^2 - |\gamma_1|^2 \quad (\text{C.2d})$$

Similarly, the  $m$ th element of the second-order derivative of  $\mathbf{a}(\theta)$  is given by

$$\begin{aligned} [\mathbf{a}''(\theta)]_m &= -j2\pi d \sin \theta \frac{m-1}{\sqrt{M}} e^{j2\pi d(m-1) \sin \theta} \\ &\quad - 4\pi^2 d^2 \cos^2 \theta \frac{(m-1)^2}{\sqrt{M}} e^{j2\pi d(m-1) \sin \theta} \end{aligned} \quad (\text{C.3})$$

Consequently, we have

$$\Re\{\gamma_2\} = -\frac{4\pi^2 d^2 \cos^2 \theta}{\sqrt{M}} \sum_{m \in S} \frac{(m-1)^2}{\sqrt{|S|}} \quad (\text{C.4a})$$

$$\Im\{\gamma_2\} = -\frac{2\pi d \sin \theta}{\sqrt{M}} \sum_{m \in S} \frac{m-1}{\sqrt{|S|}} \quad (\text{C.4b})$$

$$\|\mathbf{a}''(\theta)\|_2^2 \approx \frac{16\pi^4 d^4 \cos^4 \theta}{M} \sum_{m=1}^M (m-1)^4 \quad (\text{C.4c})$$

$$\varpi_2^2 = \|\mathbf{a}''(\theta)\|_2^2 - \Re^2\{\gamma_2\} - \Im^2\{\gamma_2\} \quad (\text{C.4d})$$

Then with  $0 < p < 1$ , we obtain

$$\gamma_0 \rightarrow \sqrt{p}, \quad \varpi_0^2 \rightarrow 1 - p; \quad (\text{C.5a})$$

$$\Im\{\gamma_1\} \rightarrow (M-1)\pi d \cos \theta; \quad (\text{C.5b})$$

$$|\gamma_1|^2 \rightarrow (M-1)^2 \pi^2 d^2 \cos^2 \theta; \quad (\text{C.5c})$$

$$\varpi_1^2 \rightarrow \frac{1}{3} M^2 \pi^2 d^2 \cos^2 \theta; \quad (\text{C.5d})$$

$$\Re\{\gamma_2\} \rightarrow -\frac{4}{3} M^2 \pi^2 d^2 \cos^2 \theta; \quad (\text{C.5e})$$

$$\Im\{\gamma_2\} \rightarrow -(M-1)\pi d \sin \theta; \quad (\text{C.5f})$$

$$\varpi_2^2 \rightarrow \frac{64}{45} M^4 \pi^4 d^4 \cos^4 \theta. \quad (\text{C.5g})$$

as  $M \rightarrow \infty$ .

## References

- [1] P. Stoica, A. Nehorai, MUSIC, maximum likelihood, and cramer-rao bound, *IEEE Trans. Acoust. Speech Signal Process.* 37 (5) (1989) 720–741.
- [2] P. Stoica, A. Nehorai, MUSIC, maximum likelihood, and cramer-rao bound: Future results and comparisons, *IEEE Trans. Acoust. Speech Signal Process.* 38 (12) (1990) 2140–2150.
- [3] F. Li, H. Liu, R.J. Vaccaro, Performance analysis of DOA estimation algorithms: unification, simplification, and observations, *IEEE Trans. Aerosp. Electron. Syst.* 29 (4) (1993) 1170–1184.
- [4] F. Li, R.J. Vaccaro, Unified analysis for DOA estimation algorithms in array signal processing, *Signal Process.* 25 (2) (1991) 147–169.
- [5] R.O. Schmidt, Multiple emitter location and signal parameter estimation, *IEEE Trans. Antennas Propag.* 34 (3) (1987) 276–280.
- [6] S. Schell, Performance analysis of the cyclic MUSIC method of direction estimation for cyclostationary signals, *IEEE Trans. Signal Process.* 42 (11) (1994) 3043–3050.
- [7] M. McCloud, L. Scharf, A new subspace identification algorithms for high-resolution DOA estimation, *IEEE Trans. Antennas Propag.* 50 (10) (2002) 1382–1390.
- [8] D. Dundu, Modified MUSIC algorithm for estimating DOA of signals, *Signal Process.* 48 (1) (1996) 85–90.
- [9] B. Rao, K. Hari, Performance analysis of root-MUSIC, *IEEE Trans. Signal Process.*, Acoust., Speech 37 (12) (1989) 1939–1949.
- [10] N. Yuen, B. Friedlander, Asymptotic performance analysis of ESPRIT, higher order ESPRIT, and virtual ESPRIT algorithms, *IEEE Trans. Signal Process.* 44 (10) (1996) 2537–2550.
- [11] M. Wax, I. Ziskind, Detection of the number of coherent signals by the MDL principle, *IEEE Trans. Acoust. Speech Signal Process.* 37 (8) (1989) 1190–1196.
- [12] L. Huang, H.C. So, Source enumeration via MDL criterion based on linear shrinkage estimation of noise subspace covariance matrix, *IEEE Trans. Signal Process.* 61 (19) (2013) 4806–4821.
- [13] L. Huang, Y. Xiao, K. Liu, H.C. So, J.K. Zhang, Bayesian-information criterion for source enumeration in large-scale adaptive antenna array, *IEEE Trans. Veh. Technol.* 65 (5) (2016) 3018–3032.
- [14] R.T. Suryaprakash, R.R. Nadakuditi, Consistency and MSE performance of MUSIC-based DOA of a single source in white noise with randomly missing data, *IEEE Trans. Signal Process.* 63 (18) (2015) 4756–4770.
- [15] J.K. Thomas, L.L. Scharf, D.W. Tufts, The probability of a subspace swap in the SVD, *IEEE Trans. Signal Process.* 43 (3) (1995) 730–736.
- [16] X. Mestre, On the asymptotic behavior of the sample estimates of eigenvalues and eigenvectors of covariance matrices, *IEEE Trans. Signal Process.* 56 (11) (2008) 5353–5368.
- [17] X. Mestre, M. Lagunas, Modified subspace algorithms for DOA estimation with large arrays, *IEEE Trans. Signal Process.* 56 (2) (2008) 598–614.
- [18] X. Mestre, Improved estimation of eigenvalues and eigenvectors of covariance matrices using their sample estimates, *IEEE Trans. Inf. Theor.* 54 (11) (2008) 5113–5129.
- [19] P. Vallet, X. Mestre, P. Loubaton, Performance analysis of an improved MUSIC doa estimator, *IEEE Trans. Signal Process.* 63 (23) (2015) 6407–6422.
- [20] B.A. Johnson, Y.I. Abramovich, X. Mestre, MUSIC, g-MUSIC, and maximum-likelihood performance breakdown, *IEEE Trans. Signal Process.* 56 (8) (2008) 3944–3958.
- [21] P. Vallet, P. Loubaton, X. Mestre, Improved subspace estimation for multivariate observations of high dimension: the deterministic signals case, *IEEE Trans. Inf. Theor.* 58 (2) (2012) 1043–1068.
- [22] P. Vallet, P. Loubaton, X. Mestre, A statistical comparison between MUSIC and G-MUSIC, in: *Proceedings of IEEE International Conference on Acoustics, Speech, and Signal Processing (ICASSP)*, 2015.
- [23] H.C. So, Y.T. Chan, K.C. Ho, Y. Chen, Simple formulas for bias and mean square error computation, *IEEE Signal Process. Mag.* 30 (4) (2013) 162–165.